PERGAMON

Atmospheric Environment 34 (2000) 925–932

ATMOSPHERIC ENVIRONMENT

www.elsevier.com/locate/atmosenv

Tropospheric LIDAR aerosol measurements and sun photometric observations at Thessaloniki, Greece

D. Balis[a,*], A. Papayannis[b], E. Galani[a], F. Marenco[a,c], V. Santacesaria[a,d], E. Hamonou[e], P. Chazette[e], I. Ziomas[a], C. Zerefos[a]

[a]*Laboratory of Atmospheric Physics, Aristotle University of Thessaloniki, P.O. Box 149, 54006 Thessaloniki, Greece*
[b]*Physics Department, National Technical University of Athens, Greece*
[c]*Italian Space Agency, Italy*
[d]*C.N.R.-I.R.O.E., Italy*
[e]*Laboratoire des Sciences du Climat et de l'Environnement (LSCE), France*

Received 23 February 1999; received in revised form 22 June 1999; accepted 13 July 1999

Abstract

We present measurements of the vertical structure of the aerosol backscattering coefficient in the lower troposphere, which have been performed at the city of Thessaloniki in N. Greece, during the years 1996 and 1997. A ground-based backscatter lidar system operated throughout the year, mostly around local noon hours. The lidar measurements were accompanied by measurements of the aerosol optical depth in the visible spectral region, using a CIMEL sun-tracking photometer. The seasonal variation of the aerosol loading and its vertical distribution in the lower troposphere over the city of Thessaloniki is discussed. The maximum values of the aerosol optical depth are found during the spring season. Indication about the origin of these maxima is given by inspection of the various aerosol layers observed in the lidar profiles. Most of the aerosol loading is present in the first 3 km height, and only in rare cases there are important aerosol layers detectable above 3 km, as in a case of Saharan dust transported over the city of Thessaloniki, in May 1997. Both instruments used in this study show similar seasonal variation of the aerosol load. It was found that almost 85% of the aerosol load is located in the layer below 3 km. There is a bias between the CIMEL and lidar derived optical depth at 532 nm, mainly attributed to the aerosols present between ground level and 600 m height, which represent up to 50% of the total aerosol optical depth.

Keywords: LIDAR; Aerosol, Optical depth

1. Introduction

Atmospheric aerosols and clouds play a substantial role in the radiative forcing of the earth's climate, as they influence the radiation balance of the Earth, mostly through scattering and absorption processes (D'Almeida et al., 1991; Ackerman and Chung, 1992; Lenoble, 1993; Chazette et al., 1999). Aerosols are produced by a variety of processes, both natural (volcanic activity, desert dust storms) and anthropogenic ones (fuel combustion, biomass burning etc.) (Lenoble, 1993; Liousse et al., 1995; Tegen and Fung, 1995). Most aerosols of anthropogenic origin are found in the lower troposphere and contribute significantly to the haze often visible during early morning hours and near sunset near the earth's surface. These aerosols have residence times of few days, and thus are distributed inhomogeneously in the atmosphere, with maximum concentrations close to their source regions (Lenoble, 1993). Presently, there are still many uncertainties concerning the spatial distribution, the shape and chemical composition of the tropospheric aerosols (Hoppel et al., 1985; Frejafon et al., 1998), and especially the chemical coupling between particulate matter and ozone.

* Corresponding author. Tel.: + 30-31-998192; fax: + 30-31-283752.
E-mail address: balis@ccf.auth.gr (D. Balis)

1352-2310/00/$ - see front matter
PII: S1352-2310(99)00317-9

The Southeastern Mediterranean region includes a variety of aerosol sources (both natural and anthropogenic) and therefore the study of the aerosols in this area is of great importance for climatic and remote sensing studies. However, very few aerosol data, based on systematic observations in this region, are currently available (Dulac et al., 1996,1997).

Extensive studies of the atmospheric aerosol load in the troposphere have been conducted the last decades using the lidar (Light Detection and Ranging) technique, mostly in the N. Hemisphere (N. America, W. Europe and in Japan) (Krueger et al., 1995; Takamura et al., 1994; Marenco et al., 1997; Papayannis et al., 1997). The lidar technique, based on the elastic backscattering of the emitted laser radiation by the atmospheric aerosols, allows the real-time visualization of the suspended particles in the atmosphere with high temporal and spatial resolution (Ferrare et al., 1991; Marenco et al., 1997). The use of tropospheric aerosols as passive tracers of the atmospheric dynamical processes, along with the appropriate experimental setup, facilitates the detailed study of the lower troposphere, by providing information on the structure and the parameters of the Planetary Boundary Layer (Ferrare et al., 1991, Kiemle et al., 1995, Papayannis and Balis, 1998).

The combined use of the lidar aerosol measurements, ancillary meteorological measurements and simultaneous measurements of the optical properties of the aerosols, can be valuable when attempting to detect atmospheric transport phenomena and diffusion properties in the lower troposphere (Hamonou et al., 1997; Dulac et al., 1997). This synergy helps to obtain quantitative information from the lidar measurements, for which several assumptions concerning the optical properties and the composition of the aerosols are necessary. Recent studies (Marenco et al., 1997; Hamonou et al., 1999) combining the use of lidar measurements with spectral solar irradiance measurements, attempt to minimize the uncertainty of the assumptions made, concerning the optical properties of the backscattering aerosols, when inverting the lidar signals. In this study aerosol optical depth measurements, performed with a commercial CIMEL sunphotometer, are used in order to help the interpretation of the lidar measurements. In Section 2 the experimental setup is presented, while in Section 3 the experimental site is described. In Section 4 the lidar inversion technique is presented, while in Section 5 the CIMEL measurements performed at Thessaloniki are described. Our results and discussion are presented in Section 6. Finally, Section 7 summarizes our conclusions.

2. Experimental setup

A ground-based backscattering lidar has been developed by the Laboratory of Atmospheric Physics (LAP) at the Aristotle University of Thessaloniki (Papayannis, 1995). The LIDAR system of LAP is a two-wavelength backscattering system pointing vertically to the zenith and is operated in the coaxial mode. A computer generated code has been applied to optimize its design and field operation (Papayannis, 1995). The system uses as an emitter a pulsed Nd : YAG laser which provides an output laser radiation at 1064 nm. It operates at a 10 Hz pulse repetition frequency and by means of frequency doubling and trippling using KD*P crystals, two wavelengths are obtained simultaneously at 532 and 355 nm. The ultraviolet and visible wavelengths are then transmitted to the atmosphere and after being backscattered from the close-range altitudes (0.5–5.5 km) they are received by a 30.5 cm diameter Newtonian telescope (1.5 m equivalent focal length). The received lidar signals are separated by a harmonic separator beamsplitter, while two narrow-band interference filters (0.1 nm FWHM at 532 and 1 nm FWHM at 355 nm), assure the reduction of the background skylight during daytime operation. In addition, two photomultiplier tubes are required for the detection of the lidar signals in both wavelengths. A complete overlap between the laser beam and the telescope's field-of-view is obtained at a range of 600 m, as has been estimated by geometrical form factor calculations performed according to Halldorsson and Langerholc (1978).

The signal acquisition, after preamplification, is performed in the analog mode by a two-channel Digitizing Oscilloscope, which acts both as a 8-bit analog-to-digital converter (ADC) and as a waveform recorder. The lidar operated for the first time in summer 1994 in Athens, Greece during the MEDCAPHOT-TRACE Campaign (Ziomas, 1998) and provided qualitative information on the boundary layer evolution, obtained by lidar, in the suburban area of Athens (Papayannis and Balis, 1998).

A Cimel CE 318 automatic suntracking photometer manufactured by CIMEL Electronique, Paris, has been installed in Thessaloniki by the Laboratoire des Sciences du Climat et de l'Environnement (LSCE). This instrument performs measurements of the optical thickness at several wavelengths in the visible spectrum and enables to assess the Angström coefficient in the same spectral region (Chazette et al., 1999). For the relevant study, the channels used are centered at 440, 670 and 870 nm, with bandwidths of less 20 nm, while the instrument field of view is about 1° (Hamonou et al., 1999).

3. Experimental site

The city of Thessaloniki (40.5°N–22.9°E) and the surrounding suburbs have close to one million inhabitants. As seen in Fig. 1, the city is developed along the Thermaikos Gulf and is northwest–southeast (NW–SE) orientated, with the sea-shore mainly on its southwest

Fig. 1. Map of the greater area of Thessaloniki, Greece.

(SW). The industrial area of Thessaloniki is located at the west–northwestern (WNW) part of the city, and includes an oil refinery complex and a chemical plant. The Laboratory of Atmospheric Physics, where the lidar and the sunphotometer are installed, is located in the down-town area, on the roof of a four-storey building at a distance of 500 m from the sea-shore and at a 60 m height above sea level (ASL). The whole northeastern part of the city is dominated by a 1-km high mountain.

4. Inversion of the lidar signals

The inversion of the lidar profiles, under the hypothesis of single scattering, for the case of a monostatic and vertically looking lidar, is based on the solution of the lidar equation (e.g. R. Collis et al., 1976):

$$P(z) = K_L \frac{\beta_R(z) + \beta_P(z)}{(z - z_L)^2} \exp\left\{ -2 \int_{z_L}^{z} [\alpha_R(z) + \alpha_P(z)]\, dz \right\}, \quad (1)$$

where $\beta_r(z)$ and $\beta_p(z)$ are the backscattering coefficients for the molecular and the particulate components of the atmosphere, respectively, and $\alpha_R(z)$, $\alpha_P(z)$ the corresponding extinction coefficients. Z_L is the altitude of the lidar system and K_L is a constant, which is characteristic for each lidar system and depends on the technical characteristics of the emitting and receiving optics.

For the lidar measurements in Thessaloniki the backward lidar inversion technique was applied (Klett, 1981,1985). In this technique, it is generally assumed that the Rayleigh extinction and backscattering coefficients are known functions of height and are obtained by the use of an atmospheric model (US Standard Atmosphere, 1976). Besides, the aerosol backscatter-to-extinction ratio C is assumed to be constant with height:

$$\beta_P(z)/\alpha_P(z) = C. \quad (2)$$

However, the ratio C depends on several parameters, such as the refractive index (which depends on the chemical composition), the size and the shape distribution of the particles. It should be stressed out that the assumption of C being independent of height, is a source of systematic error (Fernald, 1984; Klett, 1985), because changes in temperature and humidity in the atmosphere cause vertical inhomogeneity in the aerosol vertical distribution (Haenel, 1976). Of course this is true only when no other additional measurements (i.e. temperature and humidity vertical profiles) are available.

Since the assumption on the value of C is probably the most important source of systematic error in the far-end solution of the Klett inversion technique, the best choice of the value of C tends to minimize this systematic error in the retrieval of $\alpha_P(z)$ and $\beta_p(z)$. In our case the value of C was chosen equal to $0.035\ sr^{-1}$, which is an average value among those suggested for rural, urban and maritime aerosols (Browell et al., 1985; Marenco et al., 1997). Finally another assumption necessary for the Klett solution of the lidar equation is that the value of $\beta_m = \beta_R(z) + \beta_P(z)$ at a far-end reference height z_m is assumed equal to $\beta_R(z_m)$. Z_m is chosen greater than 5.5 km, by examining separately each lidar signal, and it defines the beginning of an aerosol-free region (for $z > z_m$). According to other studies, involving tropospheric lidar measurements, this assumption, in the absence of any clouds is rather realistic (Marenco et al., 1997; Santacesaria et al., 1998).

The lidar measurement accuracy concerning the retrieval of the aerosol backscattering and extinction coefficients at 355 and 532 nm has been addressed in previous papers (Chazette et al., 1995; Marenco et al., 1997). The lidar errors include the statistical and the systematic ones. In our case the statistical error in the retrieval of $\alpha_P(z)$ and $\beta_p(z)$, up to 5 km is less than 1% (Papayannis et al., 1990), since the signal-to-noise ratio (SNR) in the lidar profile is still high at that altitude ($\sim$ SNR > 3.5). The systematic error, on the other hand, is much higher than the statistical one and it strongly depends on the variability of C with altitude in the lower troposphere. However, in any case, the systematic error in the retrieval of both $\alpha_P(z)$ and $\beta_p(z)$, at 355 and 532 nm, stays below 30%, when the mean value of C is taken equal to $0.035\ sr^{-1}$ (Chazette et al., 1995; Marenco et al., 1997).

5. Description of the CIMEL measurements

The inversion of the solar radiances measured by the CIMEL sunphotometer to retrieve the aerosol optical

depth values is based on the calibration of the instrument, using the Langley plot method. The calibration of the CIMEL instrument was continuously monitored during the measuring periods. The calibration was performed on days when the atmospheric optical depth was stable from the sunrise to noon or from the noon to sunset. The total optical depth of the atmosphere at the wavelength λ is then calculated using the Beer–Lambert law (Eq. (3)), assuming that the contribution of multiple scattering within the small field of view of the sunphotometer is negligible:

$$I_\lambda = I_\lambda^0 \exp\left(-\frac{\tau_\lambda}{\mu_s}\right) \tag{3}$$

where I_λ^0 and I_λ are, respectively, the solar irradiances at the ground level and at the top of the atmosphere and μ_s is the cosine of the solar zenith angle. τ_λ is the total atmospheric optical thickness resulting from the contributions of Rayleigh scattering τ_λ^r and aerosol scattering τ_λ^a, as well as from gaseous absorption τ_λ^g (O_3 at 670 nm and H_2O at 870 nm). The aerosol optical depth at 0.532 μm was derived from the measurements in the blue and red channels using the following relation, derived from the well-known spectral dependence of the aerosol optical thickness in the visible spectrum (Angström, 1964):

$$\frac{\tau_{0.532}^a}{\tau_\lambda^a} = \left(\frac{0.532}{\lambda}\right)^{-\alpha} \tag{4}$$

where the Angström exponent is related to the aerosol size distribution (Junge, 1963).

The major source of uncertainty in the retrieval of the total aerosol optical depth is due to calibration error, which is directly proportional to the associated uncertainty on the aerosol optical depth. The relative error ε is derived from the Beer–Lambert law (e.g. Lenoble, 1993) and is given by

$$\varepsilon = \frac{1}{m}\frac{\Delta I_0}{I_0} \tag{5}$$

where $\Delta I_0/I_0$ is the relative uncertainty on the calibration coefficient and m the relative air mass. From a detailed error analysis of the CIMEL measurements performed by Hamonou et al. (1999), the error in the retrieved optical depth is less than 8%.

6. Results and discussion

The measurements presented in this paper cover the period from March 1996 to July 1997. The lidar measurements were performed regularly during this period in order to determine the background aerosol conditions in the lower troposphere over the city of Thessaloniki. In June 1996 the whole set-up was transferred to the island of St. Efstratios in Northern Aegean, while during August 1996 and between January and March 1997 the system was not operated, due to maintenance purposes. In Table 1 the measurement dates and the number of the available lidar measurements are presented. The CIMEL measurements, cover the period April 1996–June 1997. During the winter months, there are limited data due to cloudy conditions.

To study the seasonal variation of the aerosol optical depth in the visible region we examined both the lidar and CIMEL data. The lidar data measurements were integrated over two layers: 0.6–5 and 3–5 km. The lower and upper limits are determined from the system capabilities. The layer 3–5 km was chosen, in order to examine the existence of any variation of the aerosol loading in the free troposphere, above the PBL, typical of long-range transport of aerosols phenomena over the Mediterranean Sea. From all the available lidar measurements, only the ones that were performed around local noon were chosen, in order to homogenize the available data.

Fig. 2 presents the monthly mean values of the optical depth measurements as derived by integrating the inverted lidar profiles of the aerosol extinction 532 nm. The error bars represent the standard deviation of the monthly mean values, calculated from daily mean values of the measurements listed in Table 1. In order to homogenize the existing dataset the daily mean values were calculated only from measurements within 11:00–15:00 LT. All measurements shown correspond to clear sky conditions. The mean value for the optical depth at 532 nm is 0.11, which however does not include the first 600 m. During the period between September 1996–December 1996, the observed aerosol optical depth, expressed as monthly mean values, appears to have smaller values (i.e. 0.05 in September 1996, at 532 nm), than the

Table 1
Lidar measurements over Thessaloniki, during 1996–1997

Month	No. of days
Mar-96	1
Apr-96	2
Jul-96	4
Sep-96	4
Oct-96	4
Nov-96	4
Dec-96	1
Apr-97	2
May-97	6
Jun-97	4
Jul-97	2

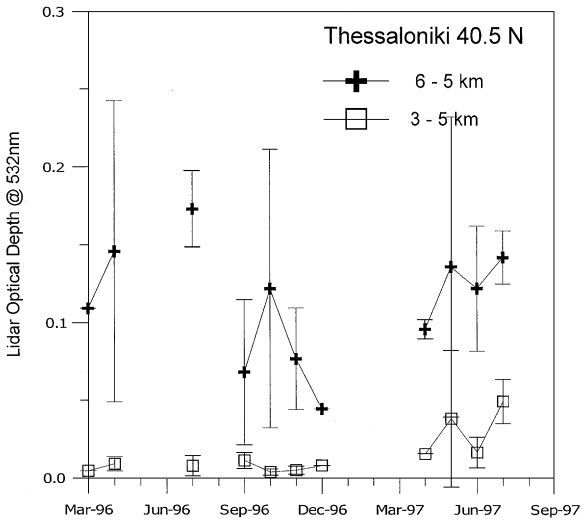

Fig. 2. Monthly mean integrated aerosol optical depth at 532 nm, derived from lidar measurements at Thessaloniki, Greece for two layers, 0.6–5 km (crosses) and 3–5 km (squares), for the years 1996–1997.

ones observed between the period from March to August 1997 (i.e. 0.15 in April 1997), except the month of October. It has to be pointed out that during the winter months clear sky conditions correspond to such synoptic conditions that result to strong northern winds. This fact limits the representativeness of the data. Comparing the different levels in Fig. 2 it is demonstrated clearly that about 85% of the aerosol load is located in the layer below 3 km. This is more pronounced during the period between September–December 1996, when this percentage exceeds 90%. However the day-to-day variability of the aerosol within a month in the 0.6–5 km layer is much larger than the one in the 3–5 km layer, where there is always a very small variability, except the case of May 1997, which is discussed in the next paragraph. The variability is larger during the transient months of autumn (October) and spring (April or May), when the prevailing weather conditions are highly variable.

In Fig. 3 the daily variation of the backscatter coefficient at 532 nm is presented, as it was observed with the lidar on 4 July 1997. As it appears from this figure, the top of the aerosol layer rises from 1.5 km, at 10:00 local time (LT) to a maximum height of $\sim$ 3 km at 16:30 LT, and later than 19:00 LT it starts to fall. The aerosol loading accumulates during the day, at heights between 1 and 2 km ASL which is represented by the higher values of the backscatter coefficient, as shown in Fig. 3. This accumulation is linked to the daily variation of the anthropogenic activities in the city and the mixing conditions, as they evolve during the day. This case study represents a typical warm summer day with moderate winds, and can provide in this way a measured estimate for the maximum expected height which can be reached

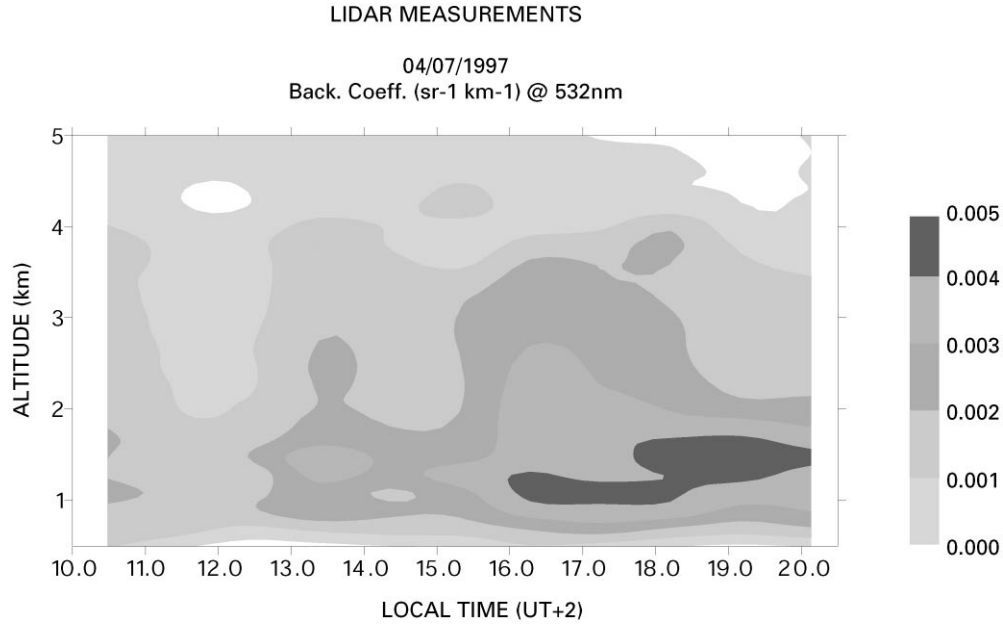

Fig. 3. Daily evolution of the vertical distribution of the aerosol backscattering coefficient at 532, for a typical summer day, at Thessaloniki, Greece.

from aerosols of local origin. The result is also supported by other case studies examined by Santacesaria et al. (1998) from the lidar measurements performed at Thessaloniki in early 1996. This fact can allow us to assign the observed aerosol variability below 3 km, presented in Fig. 2, to the variability of the local sources, both natural and anthropogenic.

In May and July 1997 relatively high values for the optical depth in the 3–5 km layer were found. These values can be possibly a result of long-range transported air masses rich in aerosol. As it is presented in detail by Hamonou et al. (1999), two cases (8–9 May and 2 June 1997) were identified from the lidar measurements, which detected the arrival of Sahara dust over Thessaloniki. This event can probably explain the larger variability of the optical depth in the 3–5 km observed in May 1997.

In Fig. 4 we compare the monthly mean aerosol optical depth measurements at 532 nm retrieved from the CIMEL sunphotometer measurements, with the integrated aerosol extinction at 532 nm as derived from the Lidar measurements. As it is shown from all the available measurements both instruments seem to retrieve similar in amplitude but not in magnitude seasonal variation for the period examined. In the same figure the monthly mean value of the Angström exponent, calculated from the visible part of the spectrum, is also shown, giving some indication for the size and the type of detected particles. The mean value of the CIMEL optical depth is 0.32 for the year 1996 and 0.26 for the first six months of the year 1997. The mean values for the Angstrom exponent are 1.6 and 1.5, respectively. These values represent carbonaceous particles, and anthropogenic or biogenic sulphates (WCP, 1983; D'Almeida et al., 1991). Larger values of the Angstrom exponent factor (> 1.6) are detected in September–October 1996 and in March–April 1997, indicating that smaller particles are detected, which probably are produced from the city activities, since these months correspond to periods with usual urban activities in the area. The period from May 1997 until July 1997, the Angstrom exponent's value is less than 1.5, indicating that larger particles like dust or mineral aerosol are also present in the atmosphere. This fact is confirmed also by the Sahara dust layers, which have been observed (Hamonou et al., 1999).

In Fig. 5 we compare simultaneous measurements with the lidar and the CIMEL instruments, performed around local noon. It is evident from this figure that 70% of the variation of the CIMEL-determined aerosol optical depth is attributed to the 0.6–5 km layer, as it appears from the simultaneous Lidar measurements. Most of the remaining variability should be attributed to the first 600 m, since the stratospheric aerosol contribution is considered negligible for the period under study. It is also evident from the fit applied to the measurements, that when the total optical thickness increases, the contribution of the aerosols in the first 600 m ASL plays a significant role to the total optical depth observed, representing up to 30% of the total aerosol optical depth.

7. Conclusions

The results from the lidar measurements performed during 1996–97 at Thessaloniki show a significant seasonal variability of the aerosol optical depth at 532 nm in the lower troposphere (0.6–5 km). The maximum values

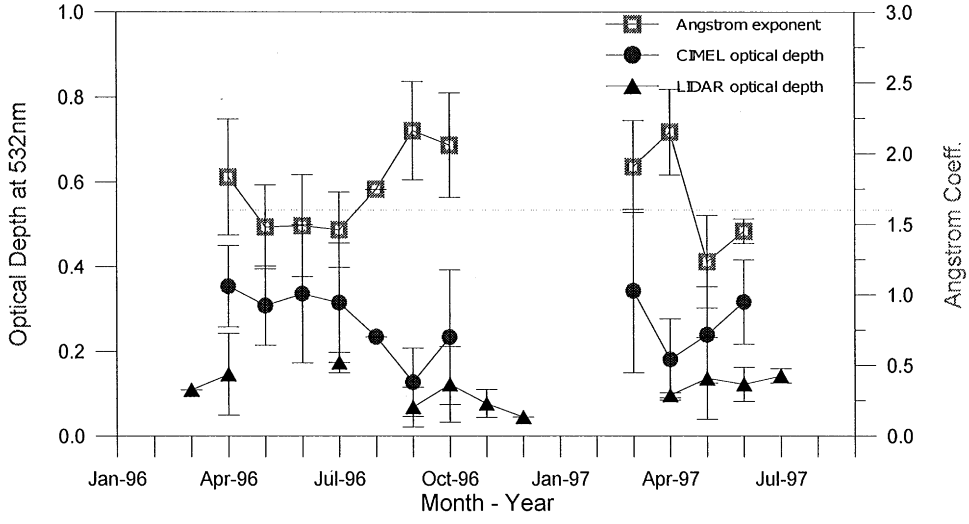

Fig. 4. Monthly mean aerosol optical depth at Thessaloniki, Greece for the years 1996–1997 derived from the CIMEL sunphotometer measurements (circles) and integrated (0.6–5 km) lidar profiles (triangles). The squares represent the monthly mean values of the Angström exponent, derived from the CIMEL measurements.

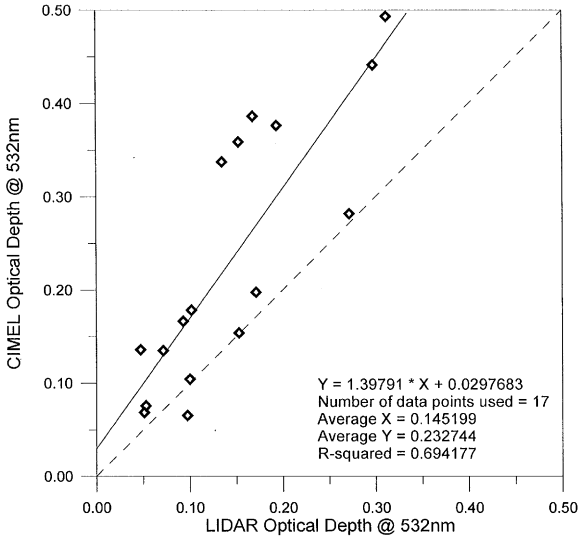

Fig. 5. Simultaneous lidar and CIMEL measurements of the aerosol optical depth at 532 nm around local noon hours, at Thessaloniki, Greece. The solid line represents the linear best fit applied to the measurements.

for clear sky conditions are found during spring, while the minimum values are observed during late autumn and winter. This variation is also confirmed from co-located CIMEL sunphotometer measurements. The aerosol loading in the 3–5 km layer represents about the 15% of the lower tropospheric aerosol, showing a very small variation through the year. The variability of the aerosol in this layer increases when long-range transport mechanisms transfer desert dust over the site. The synergy of the Lidar and sunphotometer measurements indicates that the aerosols over the measuring site are mostly carbonaceous particles and anthropogenic or biogenic sulphates. Under high aerosol optical depth conditions the first 600 m, which are not included in the Lidar measurements, represent almost 30% of the aerosol loading.

Acknowledgements

This study was financially supported by EU-DGXII MEDUSE project, Contract No ENV4-CT95-0036, and by the General Secretariat for Research and Technology (GSRT) of the Greek Ministry of Development (PENED95 project).

References

Ackerman, F., Chung, H., 1992. Radiative effects of airborne dust and regional energy budget at the top of the atmosphere. Journal of Applied Meteorology 31, 223–233.

Angström, A., 1964. The parameters of atmospheric turbidity. Tellus 16, 64–75.

Browell, E.V., Ismail, S., Shipley, S., 1985. Ultraviolet DIAL measurements of ozone profiles in regions of spatially inhomogeneous aerosols. Applied Optics 24, 2827–2836.

Chazette, P., David, C., Lefrere, J., Godin, S., Pelon, J., Megie, G., 1995. Comparative lidar study of the optical, geometrical and dynamical properties of stratospheric post-volcanic aerosols following the erruption of El Chichon and Mount Pinatubo. Journal of Geophysical Research 100, 23195–23207.

Chazette, P., Pelon, J., Dulac, F., Trouillet, V., Carrasco, I., Hamonou, E., 1999. Lidar evidence of desert dust layers in the Atlantic and Mediterranean and assessment of their infrared radiative impact. Journal of Aerosol Science, in press.

Collis, R.T.H., Russel, P.B., 1976. Lidar measurement of particles and gases by elastic backscattering and differential absorption. In: Hinkley, E.D. (Ed.), Laser Monitoring of the Atmosphere. Springer, Berlin, pp. 71–151.

D'Almeida, G.A., Koepke, P., Shettle, E.P., 1991. In: Deepak, A. (Ed.), Atmospheric Aerosols. Global Climatology and Radiative Characteristics. Hampton, VA. USA.

Dulac, F., Moulin, C., Lambert, C., Guillart, F., Poitou, J., Guelle, W., Quetel, C., Schneider, E., Ezat, U., 1996. Quantitative remote sensing of African dust transport to the Mediterranean. In: Guerzoni, S., Chester, R. (Eds.), The Impact of Desert Dust Across the Mediterranean. Kluwer Academic Publishers, Dordrecht, pp. 25–49.

Dulac, F., Hamonou, E., Schneider, X., Moulin, C., Chazette, P., Liberty, G.L., Paronis, D., Lambert, C.E., Defossez, J.-B., Balis, D., Papayannis, A., Ancellet, G., Mihalopoulos, N., 1997. Meteosat and ground-based optical measurements of desert dust within the european project MEDUSE. In Procedings EUMESTAT Conference, Brussels, 29 September 3 October 1997.

Fernald, G.F., 1984. Analysis of atmospheric lidar observations: some comments. Applied Optics 23, 652–653.

Ferrare, R., Schols, J., Eloranta, E., 1991. Lidar observations of banded convection during BLX83. Journal of Applied Meteorology 30, 312–326.

Frejafon, E., Kasparian, J., Rimbaldi, P., Yu, J., Vezin, B., Wolf, J.P., 1998. 3D analysis of urban aerosols by use of a combined lidar, scanning electron microscopy and X-ray microanalysis. Applied Optics 37, 2231–2237.

Haenel, G., 1976. The properties of atmospheric aerosol particles as a function of the relative humidity at thermodynamic equilibrium with the scattering moist air. Advances in Geophysics 19, 73–188.

Halldorsson, T., Langerholc, J., 1978. Geometrical form factors for the LIDAR function. Applied Optics 17, 240–244.

Hamonou, E., Chazette, P., Papayannis, A., Balis, D., Marenco, F., Santacesaria, V., Ancellet, G., 1997. Ground-based measurements of Saharan dust optical properties in the frame of the European MEDUSE Project. Journal of Aerosol Science 28 (Suppl. 1), S695–S696.

Hamonou E., Chazette, P., Balis, D., Dulac, F., Schneider, X., Galani, E., Ancellet, G., Papayannis, A., 1999. Local and regional scale observations of dust exports from North Africa to the Mediterranean basin in the frame of MEDUSE project. Journal of Geophysical Research, in press.

Hoppel, W., Fitzerald, J., Larson, R., 1985. Aerosol size distribution in air masses advecting off the east coast of the United States. Journal of Geophysical Research 90, 2365–2379.

Junge, C.E., 1963. Air Chemistry and Radioactivity. Academic Press Inc, New York.

Kiemle, C., Kaestner, M., Ehret, G., 1995. The convective boundary layer structure from lidar and radiosonde measurements during the EFEDA' 91 campaign. Journal of Atmospheric and Oceanic Technology 12, 771–782.

Klett, J.D., 1981. Stable analytical inversion solution for processing lidar returns. Applied Optics 20, 211–220.

Klett, J.D., 1985. Lidar inversion with variable backscatter to extinction ratios. Applied Optics 24, 1638–1643.

Krueger, D., Caldwell, L., Alvarez, H., She, C., 1995. Self-consistent method for determining vertical profiles of aerosols and atmospheric parameters using a high-spectral resolution Rayleigh-Mie lidar. Journal of Atmospheric and Oceanic Technology 10, 533–545.

Lenoble, J., 1993. In: Deepak, A. (Ed.), Atmospheric Radiative Transfer. A. Deepak Publ., Hampton VA, USA.

Liousse, C., Devaux, C., Dulac, F., Cacheir, H., 1995. Aging of Savanna biomass burning aerosols: consequences for their optical properties. Journal of Atmospheric Chemistry 22, 1–17.

Marenco, F., Santacesaria, V., Bais, A., Balis, D., di Sarra, Papayannis, A., Zerefos, C.S., 1997. Optical properties of tropospheric aerosols determined by lidar and spectrophotometric measurements (PAUR campaign). Applied Optics 36, 6875–6886.

Papayannis, A., Ancellet, G., Pelon, J., Megie, G., 1990. Multiwavelength lidar for ozone measurements in the troposphere and the lower stratosphere. Applied Optics 29, 467–476.

Papayannis, A., 1995. The EOLE project: a Greek LIDAR system for ozone and aerosol measurements in the troposphere and the lower stratosphere. Part I: Overview. International Journal of Remote Sensing 16, 3595–3604.

Papayannis, A., Ancellet, G., Barbini, R., Boesenberg, J., Calpini, B., Diehl, W., Milton, M., Del Guasta, M., Trickl, T., 1997. Large-scale European Network of laser remote sensing facilities for environmental an industrial monitoring of toxic and Global Change related trace gases (HCM Lidar Network). In: Advances in Atmospheric Remote Sensing with Lidar. Springer, Berlin, Germany, pp. 431–434.

Papayannis, A., Balis, D., 1998. Study of the structure of the lower troposphere over Athens using a backscattering lidar during the MEDCAPHOT-TRACE experiment: measurements over a suburban area. Atmospheric Environment 32, 2161–2172.

Santacesaria, V., Marenco, F., Balis, D., Papayannis, A., Zerefos, C., 1998. Lidar observations of the Planetary Boundary Layer above the city of Thessaloniki. Nuovo Cimento della Societa Italiana de Fisica 21 (6), 585–596.

Takamura, T., Sasano, Y., Hayakashi, T., 1994. Tropospheric aerosol optical properties derived from lidar, sun photometer and optical particle counter measurements. Applied Optics 33, 7132–7140.

Tegen, I., Fung, I., 1995. Contribution to the atmospheric mineral aerosol load from land surface modification. Journal of Geophysics Research 100, 18707–18726.

US Standard Atmosphere, 1976. US Goverment printing Office, Washington, DC, USA.

World Climate Programme (WCP), 1983. Aerosols and their climate effects, Series Report 55. In: Deepak, A., Gerber, H.E. (Eds.), International Council of Scientific Unions and WMO, Geneva.

Ziomas, I.C., 1998. The Mediterrenean campaign for photochemical tracers-transport and chemical evolution (MEDCAPHOT-TRACE): an outline. Atmospheric Environment 32, 2045–2053.